Microstructural characterisation of fatigue crack growth fracture surfaces of lamellar Ti45Al2Mn2Nb1B

Yang, J.; Li, H.; Hu, D.; Dixon, M.

DOI:
10.1016/j.intermet.2013.10.011

Document Version
Publisher's PDF, also known as Version of record

Citation for published version (Harvard):
Yang, J, Li, H, Hu, D & Dixon, M 2014, 'Microstructural characterisation of fatigue crack growth fracture surfaces of lamellar Ti45Al2Mn2Nb1B', *Intermetallics*, vol. 45, pp. 89-95. https://doi.org/10.1016/j.intermet.2013.10.011

Intermetallics 45 (2014) 89–95

Contents lists available at ScienceDirect

Intermetallics

journal homepage: www.elsevier.com/locate/intermet

Microstructural characterisation of fatigue crack growth fracture surfaces of lamellar Ti45Al2Mn2Nb1B

J. Yang [a,b], H. Li [b], D. Hu [a,*], M. Dixon [c]

[a] Interdisciplinary Research Centre in Materials, University of Birmingham, Edgbaston, Birmingham B15 2TT, UK
[b] School of Metallurgy and Materials Science, University of Birmingham, Edgbaston, Birmingham B15 2TT, UK
[c] Rolls-Royce Plc, Derby DE24 8BJ, UK

ARTICLE INFO

Article history:
Received 16 April 2013
Received in revised form
10 October 2013
Accepted 17 October 2013
Available online 2 November 2013

Keywords:
A. Titanium aluminides, based on TiAl
B. Fatigue resistance and crack growth
B. Fracture mode
D. Microstructure (as-cast)

ABSTRACT

Investment cast Ti45Al2Mn2Nb1B with fine lamellar microstructures was subject to fatigue crack propagation testing at 650 °C and a stress ratio of $R = 0.1$. The fracture surfaces were examined under SEM and the observed features are correlated with both stress intensity range (ΔK) and lamellar orientation. Translamellar fracture is primary fracture mode for most of the lamellar orientations. Interlamellar fracture is influenced by a combination of the ΔK and lamellar orientation. At low ΔK only the lamellar colonies with their lamellar interfaces almost perpendicular to the stress axis fractured via interlamellar fracture mode. At high ΔK interlamellar fracture can occur in lamellar colonies with any orientations.

1. Introduction

Being potential high performance high temperature structure materials TiAl-based alloys have been subjected to intensity investigation since late 1980s [1–3]. Fatigue crack propagation behaviour in TiAl alloys attracted immense attention in 1990s owing to the alloys' most likely fatigue fracture critical applications in turbines [4–15]. Research activities in this area, alongside with those in other areas in TiAl alloys, ebbed after 2000, but has revived recently to some extent with the success in certification of TiAl components in a commercial aero-engine [16–18]. Over the years many data have been accumulated and the basic understanding on the microstructure-fatigue crack propagation behaviour relationship has been established. The main findings are: a) lamellar TiAl alloys offers better crack propagation resistance than their duplex and equiaxed gamma counterparts [5,6,11,13–15], b) lamellar TiAl alloys have two major fracture modes, interlamellar and translamellar fracture [8], and c) crack propagation resistance is lamellar orientation dependent [7,10]. In spite of those important findings there are still many aspects remaining unclear. For example, in polycrystalline lamellar TiAl alloys under what conditions the specific fracture mode prevail and what is the micro-mechanism of lamellae fracture. In addition, the characterisation of the fatigue crack propagation fracture surfaces has been patchy and there was only one paper dedicated to fracture surface characterisation [8]. Therefore, many features could have been left unnoticed and they might hold important clues to the micro-mechanism of lamellae fracture during fatigue crack propagation. This paper is aimed at presenting systematic observations on the fracture surfaces of fine-grained lamellar Ti45Al2Mn2Nb1B subject to crack propagation testing at 650 °C with the attempt to relate the observed fracture surface features to the lamellar orientation and stress intensity range (ΔK).

2. Experimental

Ti45Al2Mn2Nb1B (at%), was cast into test bars using investment casting technique and the test bars were subject to a proprietary HIP and heat treatment cycle. The actual composition is very close to the nominal composition with oxygen concentration at about 600 wtppm.

The material was machined into testpieces containing a gauge length of square cross section of 5×5 mm^2. The gauge length is 25 mm. A notch was introduced at one corner of each testpiece to a depth of 0.75 mm as measured from the corner position using fine wire (ϕ30 μm) EDM cutting. Many fine cracks were generated during the re-cast process of EDM at the notch surface and they can be 10 micron in depth. The fine cracks form an almost continuous

* Corresponding author. Tel.: +44 1214147840.
E-mail address: d.hu@bham.ac.uk (D. Hu).

0966-9795/$ – see front matter © 2013 Elsevier Ltd. All rights reserved.
http://dx.doi.org/10.1016/j.intermet.2013.10.011

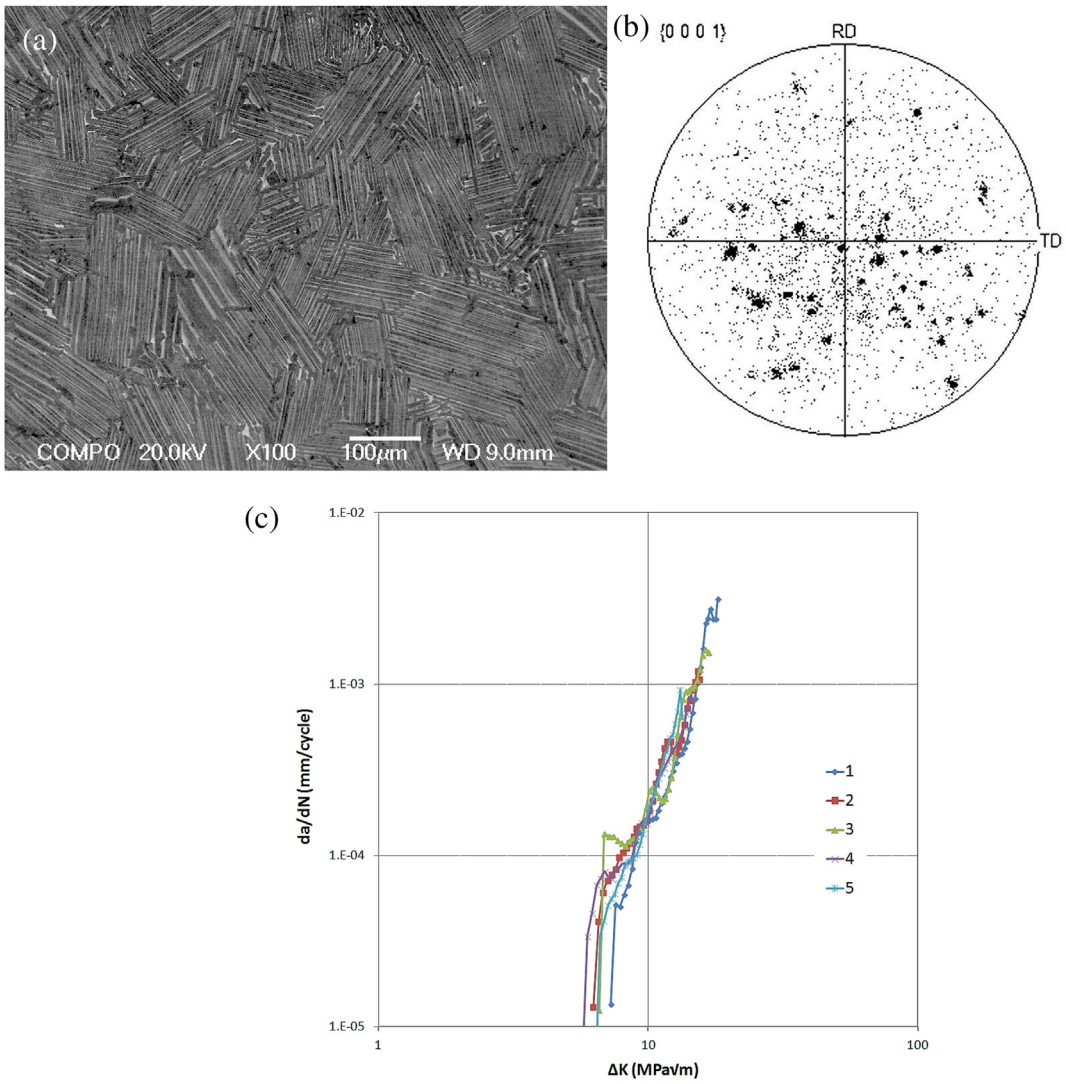

Fig. 1. (a) SEM BSE image showing the lamellar microstructure of investment cast Ti45Al2Mn2Nb1B and (b) the EBSD $(0001)_{\alpha 2}$ pole figure shows the random lamellar orientation distribution. (c) Fatigue crack propagation curves at 650 °C with $R = 0.1$.

network. During testing those with the favourable orientations will propagate under certain stress conditions. It should be noted here that using EDM cut instead of precrack is not an established conventional method. The feasibility of this method in testing TiAl alloys has been under investigation for a few years and the details will be published in a separate paper. Nevertheless, owing to the brittle nature of the TiAl alloys the measured threshold values are very close to those using precracking method under the condition of similar microstructures. Testing to determine the threshold stress intensity factor and fatigue crack growth rates was conducted under constant amplitude load at 650 °C in air. A stress ratio, R, of 0.1 and a frequency of 10 Hz were employed in all tests. Due to the brittleness and special crack growth characteristics of the material, the threshold stress intensity factor was measured directly from the EDM sharp notch by step increasing load (stress intensity factor range, ΔK) from an initial value well below the threshold. The total number of cycles spent at each load level is 5×10^4 cycles at minimum. The load was kept unchanged once consistent crack growth was observed and the crack was allowed to grow until a predetermined crack length was reached. A direct current potential difference (d.c.p.d.) technique was utilised to automatically monitoring the extension of the fatigue crack using a calibrated relationship between crack length and potential drop. After fatigue crack growth testing, samples were loaded monotonically to failure to allow a rough estimation of the fracture toughness to be made. The fracture surfaces were examined using scanning electron microscopy (SEM).

The microstructure of the alloy is shown in Fig. 1(a) and is composed of fine lamellar colonies with an average lamellar colony size of about 100 μm determined using linear intercept method and a maximum grain size of 240 μm. The lamellar colony orientation was measured using electron back-scattering diffraction (EBSD) and the (0001) pole figure of the alpha2 phase is shown in Fig. 1(b). Owing to the fact that each lamellar colony descended from one prior alpha grain, the orientation of each $(0001)_{\alpha 2}$ spot is the orientation of the lamellar interfaces in each colony. Thus, it is shown by this pole figure that the lamellar colonies are randomly oriented. The orientation of the fracture surface images in this paper is as that the stress axis is perpendicular to the images and the overall crack propagation direction is upwards for Figures 3, 5–7.

Fatigue crack growth rate (da/dN) versus stress intensity factor range (ΔK) curves of 5 testpieces are shown in Fig. 1(c). At 650 °C in air the threshold stress intensity factor range (ΔK_{th}) is measured to

be between 6 and 7 MPa√m with the R ratio of 0.1. Once the threshold is exceeded the fatigue crack growth rate increases sharply with the increase of ΔK demonstrating a cliff edge appearance of the curves at the near threshold region. This characteristic is commonly seen at elevated temperatures in TiAl alloys.

3. Results

3.1. Overview

The overview of the typical fracture surface along the diagonal of a broken testpiece is shown in Fig. 2 with the crack growth direction from right to left. Starting from the right edge Fig. 2 shows a straight notch front, a large area of fatigue crack growth and a final monotonic tensile fracture area. The boundary between the fatigue and tensile fracture regions can be easily identified under optical microscopy through different shades of discolouration caused by oxidation, which cannot be seen under SEM. However the SEM images bring out the topological contrast which is very subtle but still distinguishable for the investigated material. The fatigue region in Fig. 2 spans a ΔK range from approximately 7 MPa√m right ahead of the EDM notch to 18 MPa√m at the end of fatigue. Two major fracture modes, interlamellar fracture and translamellar fracture, have been observed. No striation, which is the signature of stable fatigue crack growth in ductile materials, can be observed in the fatigue zone.

3.2. Interlamellar fracture

Interlamellar fracture was found throughout the fracture surfaces and the facets could have contrast darker or brighter than other areas in secondary electron SEM images, depending on their orientations. Those parallel to or having small angles with the fracture plane appear darker whilst those appearing like cliffs in the images, are often brighter than their surroundings. More facets can be seen at the left side (high ΔK region) of the image than at the right side (low ΔK region) in Fig. 2. The cliff-like facets are difficult to see in low magnification SEM images. Fig. 3 shows two examples of interlamellar fracture surfaces from two lamellar colonies with an angle of about 50–60° off the stress axis.

Pole figure is used to describe the orientation of lamellar colonies on the fracture surface and the three axes are defined as such that the centre is the applied stress direction, N, the A axis is at the top of the pole figure for the overall crack propagation direction and to the right of the pole figure is the B axis, as shown in Fig. 4. The orientation of the colonies is represented by the poles of their lamellar interface normal in the pole figures. The orientation of a lamellar colony can be described by two angles shown in Fig. 4(b) for the pole labelled '16.1'. The first is the angle between lamellar interface normal and the N axis, here referred to as the 'Orientation' for simplicity. The second angle, an acute angle, is that between the projection of lamellar interface normal onto the fracture plane and the A axis, reflecting the relation between the lamellar interfaces and the overall crack propagation direction. It is referred to as the 'Sub-Orientation' in this work.

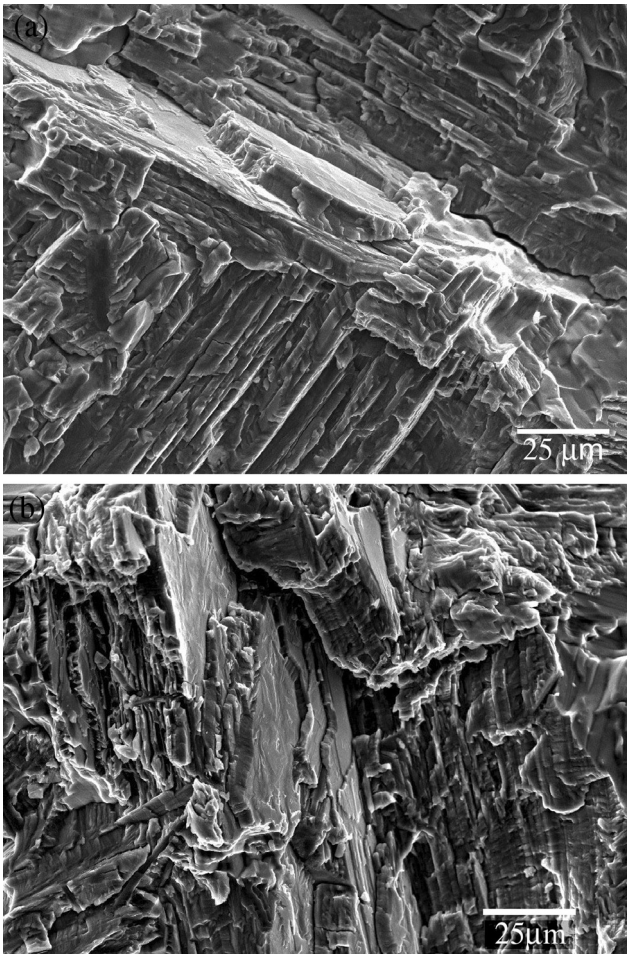

Fig. 3. Interlamellar fracture at high ΔK; (a) 15.3 and (b) 14.1 MPa√m.

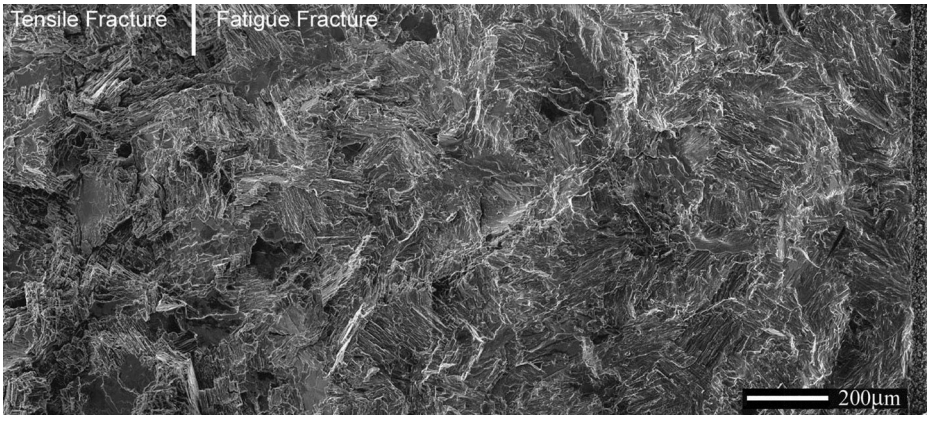

Fig. 2. SEM montage showing the fracture surface of a sample tested at 650 °C. The fatigue crack propagation direction is to the left and the range of the ΔK is 7–18 MPa√m.

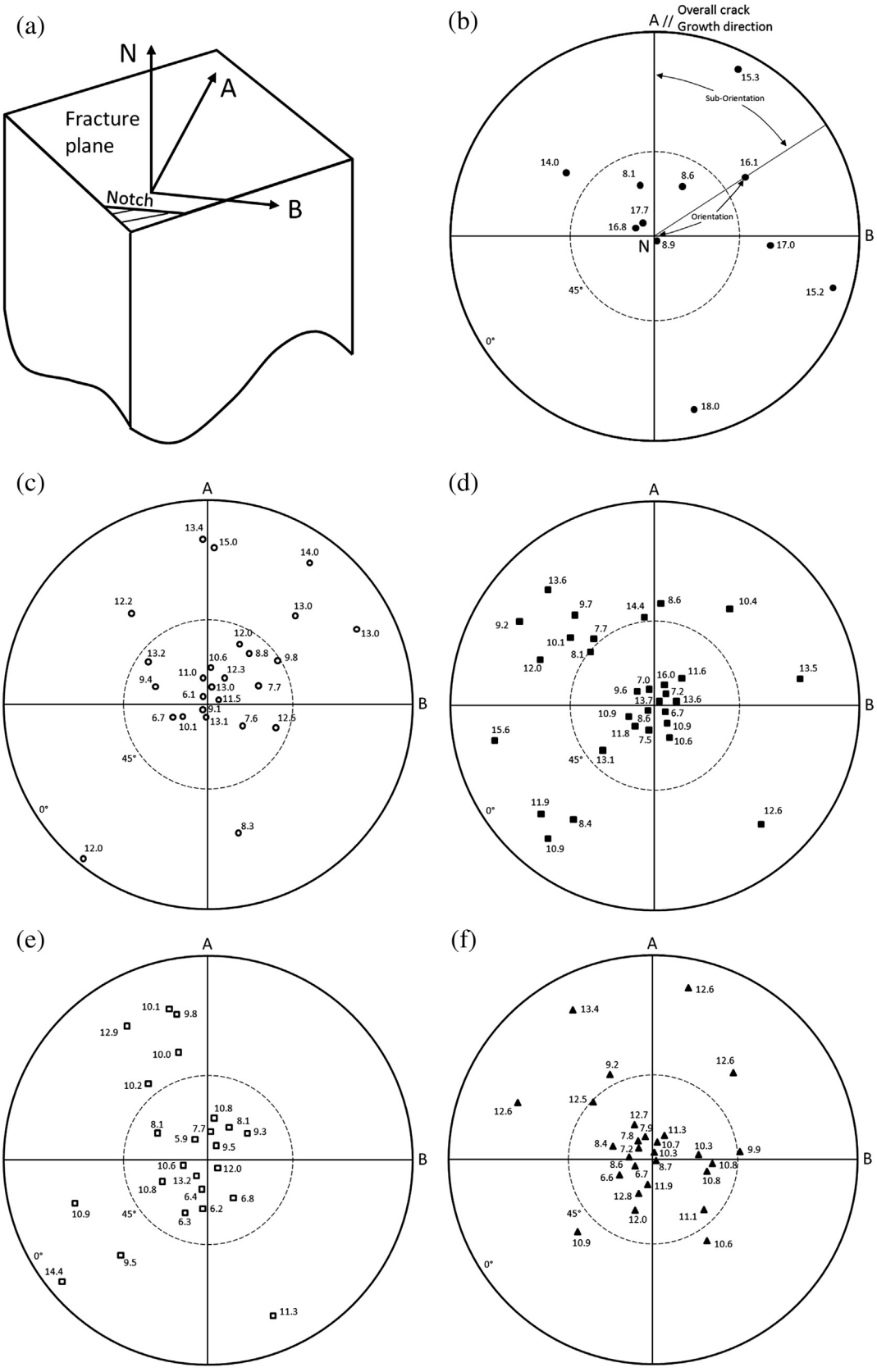

Fig. 4. (a) Definition of pole figure directions with respect to the stress axis and the fracture plane. (b)–(f) Pole figures showing the orientations of interlamellar-cracked colonies observed on the fracture surfaces of 5 samples together with their local stress intensity range.

Thus, the two interlamellar cracking facets in Fig. 3 have similar Orientations but very different Sub-Orientations. The former is nearly facing the overall crack propagation direction and the latter is almost perpendicular to it. The orientation of interlamellar-cracked colonies in the fatigue zones was measured in a SEM using an image rotation method. The sample stage was rotated to maximise or minimise the shown area of a specific facet and the orientation of this facet (lamellar interface) can be worked out from the rotations with an accuracy of about 5°. The results from 5 samples are shown in pole figures in Fig. 4(b–f), in which each dot represents the normal of a facet from an interlamellar-cracked colony. The stress intensity range ΔK of each colony is given next to its pole. It is noted here that the stress intensity range for specific points on the fracture surfaces was obtained through linear interpolation between two measured crack lengths which were determined using d.c.p.d method. This method is unable to guarantee the accuracy to the first decimal point of the stress intensity range values. Therefore, the results shown here should be treated as qualitative or semi-quantitative at most.

A few points are highlighted by the pole figures. Firstly the lamellar colonies with Orientations close to 0° can be fractured in interlamellar fracture mode at both high and low ΔK levels. Secondly cliff-like interlamellar fracture (the fractured colonies with high angle Orientations) only occurred at high ΔK level and finally, changing the Sub-Orientation while keeping the Orientation constant makes almost no difference in interlamellar cracking behaviour. It can be affirmed that the occurrence and fracture surface morphology of interlamellar fracture is related to lamellar orientation AND stress intensity range ΔK. At low ΔK (up to 9–10 MPa$\sqrt{m}$, based on the observation of about 10 specimens) interlamellar cracking only occurs in the colonies with their lamellar interfaces perpendicular to the stress axis with a deviation up to ~30°. Results from all 5 analysed samples show the same characteristics although the ΔK range of each of them is slightly different.

3.3. Translamellar fracture

Translamellar fracture occurred throughout the whole fracture surfaces and it is the primary fracture mode. It was found in this study that the fracture surface morphology differs with the stress intensity range ΔK. Fig. 5 shows the translamellar fracture surface morphology at low ΔK (7.5, 6.4 and 6.5 MPa$\sqrt{m}$ for 5a, 5b and 5c respectively). The three colonies have high angle Orientations with different Sub-Orientations (being A, B and AB respectively). The fracture surfaces are fairly smooth, compared to those observed at high ΔK values such as those in Fig. 6, regardless of their Sub-Orientations. There are some fine linear features lying across the lamellae and those within the same lamella are almost parallel to each other. Those linear features bear no relation with the overall crack propagation direction and are more likely to be related to their own crystalline structures [19]. Also it should be noted that the lamellar interfaces are intact and free from secondary cracking.

The morphology of the facture surfaces at high ΔK is very different. Fig. 6 shows two translamellar-cracked colonies at ΔK values of 15.5 and 16.2 MPa$\sqrt{m}$. Again, both of them have high angle Orientation and the one in Fig. 6(a) has ~80° Sub-Orientation and the other is about 30° from the A direction. The fracture surfaces are very rough. The roughness was caused by the large steps formed by secondary interlamellar cracking (two deep vertical interfacial cracks in Fig. 6(a)) and small steps within/along each lamella. The small steps were not observed during fracture at low ΔK. At high ΔK interlamellar fracture occurs simultaneously as the secondary cracking in the lamellar colonies while cracks grow predominantly in translamellar fracture manner.

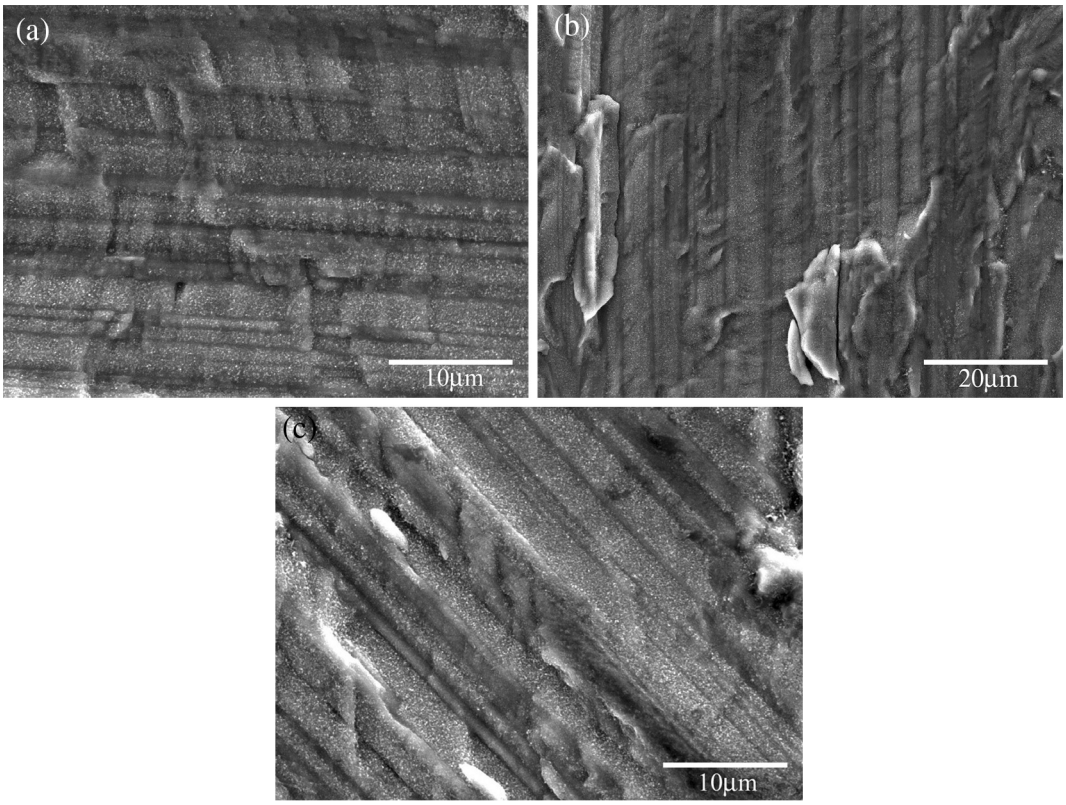

Fig. 5. Translamellar fracture at low ΔK; (a) 7.5, (b) 6.4, and (c) 6.5 MPa$\sqrt{m}$.

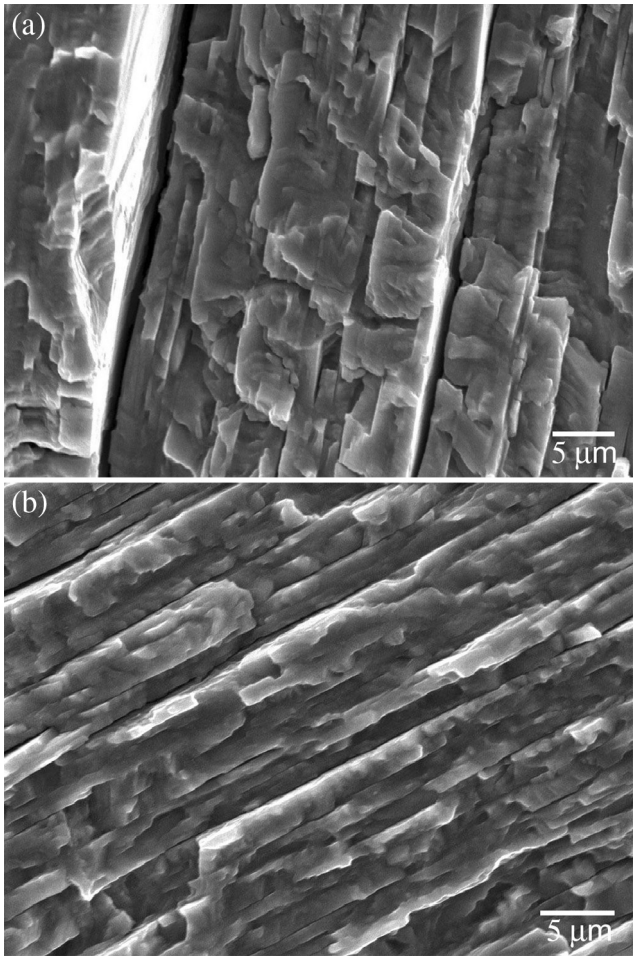

Fig. 6. Translamellar fracture at high Δ*K*; (a)15.5 and (b) 16.2 MPa√m.

3.4. Other fine features

An interesting observation is the transversal ridges (with respect to the lamellar interface traces) on the translamellar-fractured colonies adjacent to interlamellar-fractured colonies. Fig. 7(a) shows an interlamellar-fractured colony right next to a notch and it is surrounded by a few translamellar-fractured colonies. The colony in the middle has a faceted fracture surface. Some ridges are on the fracture surfaces of those surrounding colonies and they are arranged in a way of radiating out from the facet. Such ridges on fracture surfaces usually are an indication of direction of the actual crack propagation and the convergent point of the ridges would be the source of cracking. Thus, it is strongly suggested that in this image the colony in the middle (with an Orientation close to 0°) cracked first and then propagated into the surrounding colonies.

Fig. 7(b) shows the ridges on the fracture surface of a translamellar-cracked colony next to/below an interlamellar-cracked colony. From the direction of the ridges it can be judged that the actual crack front moved downward (shown with the white arrow) which is opposite to the overall crack propagation direction. Fig. 7(c) shows a case of cracking within a lamellar colony with an Orientation of about 30°. Cracking within this colony occurred on lamellar interfaces at different depths and the crack torn through the lamellae between them. All the cracked lamellar interfaces are shown as facets. A high magnification image of the area just under 'A' in Fig. 7(c) is given in Fig. 7(d) where a river pattern can be seen clearly. This river pattern tells that the local crack front moved downwards along the white arrow. Therefore in this colony the crack on lamellar interface A should have been fractured first and moved onto interfaces at B via tearing through the lamellae between A and B. Again, the actual local crack front moving direction is different to the overall crack propagation direction.

4. Discussion

Lamellar TiAl alloys are brittle in nature and a large part of their shown ductility (up to 2% before brittle–ductile transition) is accompanied by cracks. Unlike in ductile materials where plastic deformation can be achieved to a large extent before formation of voids and cracks, cracking in lamellar TiAl alloys occurs at the very beginning of plastic deformation. An earlier study revealed that the first detected cracking under monotonic tension was at about 2/3–3/4 of the 0.2% proof stress, which is just above the elastic limit [20]. This is an intrinsic feature of the lamellar TiAl alloys arising from both limited slip systems in the $L1_0$ gamma phase and the low interface transparency for slip transfer between lamellae [21]. In such lamellar structures interfacial cracking is the most effective way to accommodate deformation discontinuity from cross-lamella slips. As a consequence the fracture surface of TiAl alloys commonly comprises interlamellar facets, typically up to the full size of the related colonies, under monotonic loading. The fracture surface of lamellar TiAl alloys under fatigue loading are in general analogous with those under monotonic loading condition, which is similar to other brittle materials such as ceramics. This observation obtained in this study is in agreement with early findings [22].

Nonetheless the fracture surfaces from fatigue crack propagation test have their own characteristics and of the most importance is the relationship between the fracture modes (interlamellar fracture and translamellar fracture) and the stress intensity range Δ*K* and lamellar orientation. The observations that there are more interlamellar cracking facets in the region with high Δ*K* than in the region with low Δ*K*, as shown in Fig. 2, and the fact that at low Δ*K* interlamellar cracking only occurred in the lamellar colonies with very low angle Orientations, as shown in Fig. 4, led to the notion that translamellar prevails at low Δ*K*. It seems that at low Δ*K* the intrinsic coherence stresses of lamellar interfaces are enough to overcome the applied stress component causing interface debonding unless the applied stress direction is close to the interface normal. The morphology of interlamellar cracking is also affected by lamellar orientation and the stress intensity range.

The local cracking direction opposite to the overall crack propagation direction shown in Fig. 7 was resulted from the interlamellar fracture in front of the main crack during fatigue testing. The crack propagates sideway and/or backward to sever the ligament in between. This is a prominent feature of fracture in lamellar TiAl alloys if not unique. This phenomenon was already reported in some early work in which the observation was made on the sides of testpieces and they were only observed on the sample surfaces [13]. What presented in this work shows the evidence of interlamellar crack in front of the main crack from the actual fracture surfaces well inside the samples.

The effect of stress intensity range on fatigue fracture surface morphology was recognised in early work but not studied in detail [8,23]. James observed that interlamellar cracking in translamellar-fractured colonies only at high Δ*K* which is the same as in this work. However, the very smooth fracture surfaces of translamellar-fractured colonies, as shown in Fig. 5, at low Δ*K* were reported here for the first time. Understanding this phenomenon is important since all those smooth fracture surfaces were found next to the notch where the Δ*K* is low and close to the threshold. In view of the fact that the observed notch areas in this work were primarily

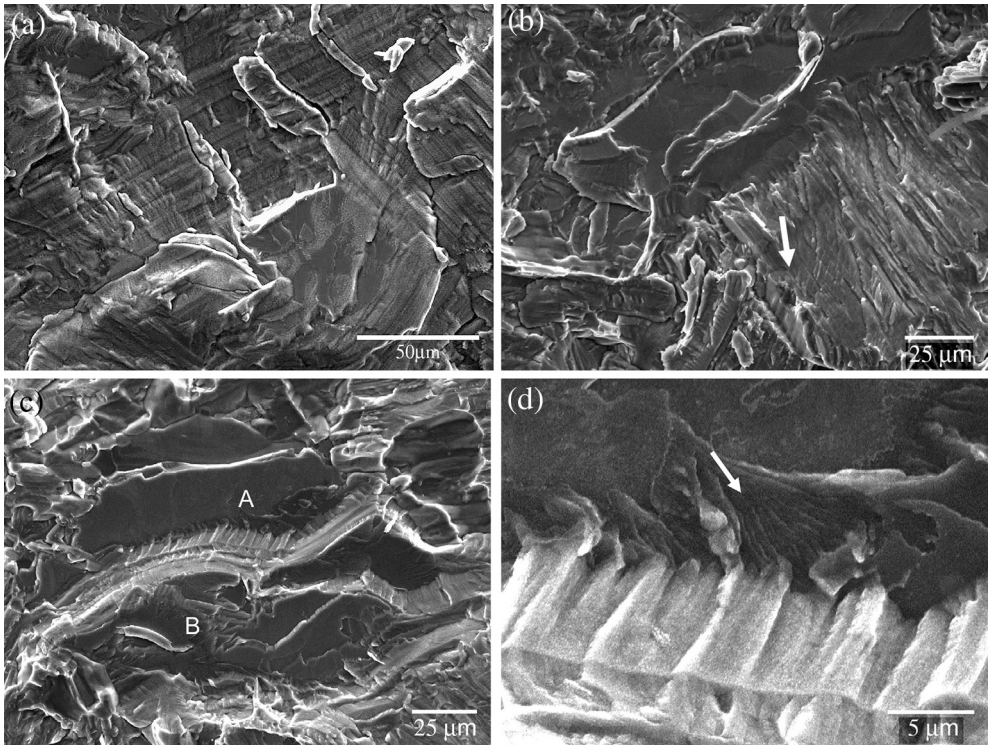

Fig. 7. Linear features on the translamellar fracture surfaces adjacent to interlamellar fracture areas. ΔK = (a) 6.3, (b) 10.2, and (c) 8.9 MPa$\sqrt{m}$.

fractured via translamellar mode and the easiness of translamellar fracture in such a smooth manner should dictate the threshold.

Interlamellar cracking within colonies is easy and fast, i.e. the crack growing across the whole lamellar colony almost instantaneously. Therefore it could not offer as much cracking resistance by itself as does the translamellar cracking. However it may diversify the local crack propagation direction, changing the Mode I cracking to mixed-mode cracking. Also the formation of interlamellar cracks in front of the main crack may dissipate energy which may help reducing crack growth rates.

The observed difference in the efficacy of influencing cracking mode by the Orientation and Sub-Orientation of lamellar colonies may came at a surprise. The Sub-Orientation of the lamellar colony showed little effect on the cracking mode which the Orientation demonstrated a dominating role together with the local stress intensity range. The difference in the two orientations may come from their relationship with the activation of slip/twinning systems. It can be worked out easily that the Orientation affects the Schmid Factor of the slip/twinning systems in the lamellae whilst the Sub-Orientation does not.

5. Summary

The main findings of this work are summarised as following:

The fracture surfaces of lamellar Ti45Al2Mn2Nb1B subjected to fatigue crack propagation testing at 650 °C in air with $R = 0.1$ are similar to those from monotonic tensile test, featured mainly with interlamellar cracking and translamellar cracking.

The operation of the fracture modes was dictated by both lamellar orientation and stress intensity range ΔK. At high ΔK interlamellar fracture occurred in colonies with any orientation whilst at low ΔK it only occurred in colonies with lamellar interface normal close to stress axis. The combination of interlamellar cracking and translamellar cracking within the same colonies forms different fracture surface features.

Acknowledgement

Financial support from the EPSRC through the Strategic Partnership is gratefully acknowledged. JY would like to thank the EPSRC for the Dorothy Hodgkin Postgraduate Awards (DHPA GAS0206).

References

[1] Lipsitt HA. JOM 1987;39(7):6.
[2] Kim Y- W. JOM 1995;47(7):39.
[3] Yamaguchi M, Inui H, Ito K. Acta Mater 2000;48:307.
[4] Soboyejo WO, Deffeyes JE, Aswath PB. Mater. Sci. Eng. A 1991;A138:95.
[5] James AW, Bowen P. Mater. Sci Eng. A 1992;A153:486.
[6] Davidson DL, Campbell JB. Met. Trans.. A 1993;24A:1555. n P. Bowen.
[7] Bowen P, Chavel RA, James AW. A192/193:443. Mater. Sci. Eng. A 1995.
[8] Balsone SJ, Worth BD, Larsen JM, Jones JW. Scripta Metall. Mater 1995;32:1653.
[9] Soboyejo WO, Aswath PB, Mercer C. Scripta Metall. Mater 1995;33:1169.
[10] Henaff G, Bittar B, Marbru C, Petit J, Bowen P. Mater. Sci. Eng. A 1996;219:212.
[11] Worth BD, Larsen JM, Balsone SJ, Jones JW. Metall. Mater. Trans.. A 1997;28A:825.
[12] McKelvey AL, Venkateswara Rao KT, Ritchie RO. Scripta Mater 1997;37:1797.
[13] Chan KS, Shih DS. Metall. Mater. Trans.. A 1998;29A:73.
[14] Gloanec A-L, Henaff G, Bertheau D, Belaygue P, Grange M. Scripta Mater 2003;49:825.
[15] Henaff G, Gloanec A- L. Intermetallics 2005;13:543.
[16] Appel F, Paul JDH, Ohering M. Gamma Titanium Aluminide Alloys. Weinheim, Germany: Wiley-VCH; 2011p1.
[17] Filippini M, Beretta S, Patriarca L, Pasquero G, Sabbadini S. Procedia Engineering 2011;10:3677.
[18] Mine Y, Takashima K, Bowen P. Materials Mater. Sci. Eng. A 2012;A532:13.
[19] Huang Z, Bowen P. Scripta Mater 2001;45:931.
[20] Hu D, Huang A, Jiang H, Mota-Solis N, Wu X. Intermetallics 2006;14:82.
[21] Hu D, Loretto MH. Intermetallics 1999;7:1299.
[22] Ritchie RO. International Journal of Fracture 1999;100:55.
[23] James AW. PhD thesis 1996. University of Birmingham.